Food & Function

ROYAL SOCIETY OF CHEMISTRY

PAPER

View Article Online
View Journal | View Issue

Cite this: *Food Funct.*, 2023, **14**, 7270

(*R*)-8-Methylsulfinyloctyl isothiocyanate from *Nasturtium officinale* inhibits LPS-induced immunoinflammatory responses in mouse peritoneal macrophages: chemical synthesis and molecular signaling pathways involved†

Manuel Alcarranza, *[a,b] Isabel Villegas,[a,b] Rocío Recio, [c] Rocío Muñoz-García, [a,b] Inmaculada Fernández [c] and Catalina Alarcón-de-la-Lastra*[a,b]

Received 19th May 2023,
Accepted 5th July 2023

DOI: 10.1039/d3fo02009f

rsc.li/food-function

The aim of this study was to develop an optimal synthetic route to obtain natural (*R*)-8-methylsulfinyloctyl isothiocyanate (**(*R*)-8-OITC**), present in watercress, based on the "DAG methodology" as well as to evaluate its potential antioxidant and immunomodulatory effects, exploring possible signaling pathways that could be involved in an *ex vivo* model of murine peritoneal macrophages stimulated with LPS. Treatment with **(*R*)-8-OITC** inhibited the levels of pro-inflammatory cytokines (IL-1β, TNF-α, IL-6, IL-17 and IL-18), intracellular ROS production and expression of pro-inflammatory enzymes (COX-2, iNOS and mPGES-1) through modulation of the expression of Nrf2, MAPKs (p38, JNK and ERK) and JAK/STAT, and the canonical and non-canonical pathways of the inflammasome. Taking all these together, our results provide a rapid and cost-effective synthetic route to obtain natural **(*R*)-8-OITC** and demonstrate that it could be a potential nutraceutical candidate for managing immuno-inflammatory pathologies. Therefore, further *in vivo* trials are warranted.

1. Introduction

Nasturtium officinale (watercress) is an aquatic or semi-aquatic perennial cruciferous herb native to Asia, Europe and North Africa. Watercress as a medicinal plant has its origins in the ancient and traditional medicines of Iran, where it is used to treat pathologies such as renal colic, hypertension and hyperglycemia.[1] In the literature, the different biological activities of this plant extract are described, such as cardioprotective,[2,3] hypolipidemic,[4] anticancer,[5–9] antioxidant,[2,10–15] anti-inflammatory,[10,12,15–17] antidiabetic,[18] antibacterial,[19,20] anti-allergic,[21] and antipsoriatic activities,[22] as well as its effects on the reproductive system.[23]

In addition to its use as a medicinal substance, watercress has shown interesting activities in the field of cosmetics due to its anti-ageing, skin-brightening and anti-acne effects, in phytoremediation and at a nutritional level, because it is currently becoming one of the most interesting vegetables in healthy diet and in modern cuisine.[1]

As a member of the Brassicaceae family, it possesses in its composition polyphenols (phenolic acids, flavonoids and proanthocyanins), pigments (chlorophylls, lycopene and carotenoids), glucosinolates (GLs) and isothiocyanates (ITCs). In addition, watercress contains a considerable amount of nutrients such as proteins, soluble sugars and vitamins.[24–27]

One of the most studied metabolites within this plant are GLs, which are the precursors of ITCs, organosulphur compounds distinguished by the existence of a β-D-thioglucosidic linkage that is coupled to D-glucose. The bioconversion of GLs into active ITCs is regulated by the presence of an endogenous myrosinase, a β-thioglucosidase which is activated upon tissue disruption, *i.e.* mastication or trituration as part of the plant defense mechanism generating ITCs and other degradation substances such as hydrolysis products. The proportion of each glucosinolate (GL) hydrolysis compound depends mostly on pH, ferrous ion and temperature conditions. Under physio-

[a]*Department of Pharmacology, Faculty of Pharmacy, Universidad de Sevilla, 41012 Sevilla, Spain. E-mail: malcarranza@us.es, villegas@us.es, rmgarcia@us.es, calarcon@us.es; Tel: +34 954559877*
[b]*Instituto de Biomedicina de Sevilla, IBiS (Universidad de Sevilla, HUVR, Junta de Andalucía, CSIC), Seville, Spain*
[c]*Departamento de Química Orgánica y Farmacéutica, Facultad de Farmacia, Universidad de Sevilla, 41012 Sevilla, Spain. E-mail: rrecioj@us.es, inmaff@us.es*
† Electronic supplementary information (ESI) available. See DOI: https://doi.org/10.1039/d3fo02009f

logical pH conditions, the major hydrolysis products are ITCs, which are considered to be responsible for the biological activity of these plants.[28–30]

With regard to watercress (*Nasturtium officinale*), one of the ITCs that is present is (*R*)-8-methylsulfinyloctyl ITC ((***R*)-8-OITC**), only a few studies have reported its activity.[1,31] **(*R*)-8-OITC** (hirsutin) is a structural analogue of sulforaphane (SFN), which has a longer aliphatic chain and is found naturally in the form of GL (glucohirsutin), as indicated in Chart 1. In particular, hirsutin has been shown to be a potent inducer of phase II enzymes of xenobiotic metabolism, and could have a potential use in cancer chemoprevention.[32,34] Hirsutin has also been shown to augment the activity and expression of the detoxifying NADPH quinone oxidoreductase, showing cytotoxicity in hepatoma cells.[35]

Taking into account that, to date, the majority of biological studies are based on plant extracts, it should be pointed out that in these cases, the amount of ITC obtained is not exactly known and the extract can contain other sub-products from the plant. Furthermore, in the process of scaled industrialisation, an exorbitant amount of vegetables should be used.

In this sense, based on our synthetic experience, we decided to synthesize the natural enantiomer of hirsutin, **(*R*)-8-OITC**, in order to obtain this ITC in large quantities and with high purity, which allows us to carry out anti-inflammatory studies with an exact sample concentration.

Fortunately, a few years ago, our research group developed an approach, "the DAG methodology", for the synthesis of enantiomerically pure sulfoxides.[36,37] Applying this methodology, in this work, we describe the first enantioselective synthesis of **(*R*)-8-OITC**, from a carbohydrate derivative (diacetone-D-glucose) as an inexpensive starting material. The synthesised compound was biologically tested in a preclinical model of murine peritoneal macrophages.

Macrophages are considered to be important agents in the inflammatory process, playing a crucial role in the immune-inflammatory response taking part in innate immunity.[38] One of the most potent initiators of inflammation is bacterial lipopolysaccharide (LPS), the major endotoxin present in the outer membrane of Gram-negative bacteria that targets Toll-like receptor 4 (TLR4) receptors on macrophages, causing a change in the cell's energy metabolism, leading to an increase in reactive oxygen species (ROS) as a result of suppressed oxidative phosphorylation and increased glycolysis.[39]

As a result of the activation of this pathway, there is an overexpression of pro-inflammatory enzymes such as inducible nitric oxide synthase (iNOS), cyclooxygenase-2 (COX-2) and microsomal prostaglandin E synthase (mPGES)-1, involved in the production of nitric oxide (NO) and prostaglandins (PGs), respectively.[40]

Additionally, the exposure of these immune cells to LPS also results in the overproduction of Th1 and Th17 pro-inflammatory cytokines, generated by the activation of several signaling pathways, including mitogen activated protein kinases (MAPKs), the inflammasome and the Janus kinase/signal transducer and activator of transcription (JAK/STAT) pathways.[33,41]

While several studies have described the anti-inflammatory and antioxidant effects of *N. officinale*, there is limited information on the pharmacological activity of **(*R*)-8-OITC**.[15–17] Considering that most probably all natural methylsulfinyl analogues exist as a single enantiomer with an R_S absolute configuration,[42] we decided to focus on the study of the biological activity of **(*R*)-8-OITC** related to its anti-inflammatory effect.

For this reason, the main objective of this study was to synthesise **(*R*)-8-OITC** in a novel way and evaluate its anti-inflammatory and antioxidant activities in LPS-induced murine peritoneal macrophages by identifying the mechanism of action and signaling pathways involved.

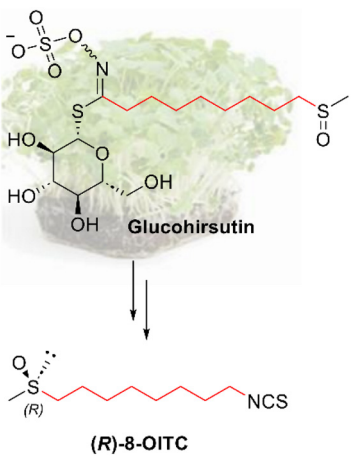

Chart 1 Molecular structure of the natural enantiomer of hirsutin (**(*R*)-8-OITC**) and its corresponding GL, glucohirsutin.

2. Materials and methods

2.1. Chemicals

2.1.1. Reagents and instruments. For reactions which were run under an atmosphere of dry argon, oven-dried glassware and dried solvents were used. Chemicals were obtained from commercial sources and used without further purification. TLC was carried out on silica gel GF254 (Merck) and compounds were detected by charring with phosphomolybdic acid/EtOH. For flash chromatography, Merck 230–400 mesh silica gel was used. Chromatographic columns were eluted with a positive pressure of air, and eluents are given as volume to volume ratios (v/v). NMR spectra were recorded using Bruker Avance 500 MHz spectrometers. Chemical shifts are reported in ppm, and coupling constants are reported in Hz. High-resolution mass spectra (HRMS) were recorded in the Centro de Investigación, Tecnología e Innovación in the University of Seville, using a Kratos MS-80RFA 241-MC apparatus. Optical rotations were determined using a PerkinElmer 341 polarimeter. Enantiomeric excesses were measured using a Waters Alliance 2695 apparatus and an Agilent Technologies 1200

series apparatus with stationary chiral phase columns (Chiralcel®).

2.1.2. 8-Azidooctan-1-ol (2). To a solution of 8-chloro-1-octanol **1** (7.2 mL, 41.75 mmol) in dry DMF (30 mL) under an atmosphere of argon, sodium azide (5.4 g, 83.50 mmol) was added. The reaction mixture was heated to 50 °C overnight. After completion of the reaction, water (20 mL) was added and extracted with CH_2Cl_2 twice. The resulting organic layers were dried over anhydrous Na_2SO_4, and the solvent was evaporated to give 7.1 g (41.60 mmol, quantitative yield) of **2** as a colorless oil, which was used without further purification. R_f = 0.15 (EtOAc/hexanes, 1 : 4); ^{1}H NMR (500 MHz, $CDCl_3$), 3.61 (t, 2H, J = 6.6 Hz), 3.23 (t, 2H, J = 7.0 Hz), 1.66 (bs, 1H), 1.60–1.51 (m, 4H), 1.38–1.32 (m, 4H) ppm (Fig. S1†); ^{13}C NMR (125 MHz, $CDCl_3$) δ 63.0, 51.5, 32.8, 29.3, 29.2, 28.9, 26.7, 25.7 ppm (Fig. S2†); HRMS (ESI) calcd for $C_8H_{17}ON_3Na$ $(M + Na)^+$ m/z 194.1264, found m/z 194.1261.

2.1.3. 8-Azidooctyl methanesulfonate (3). To a solution of 8-azidooctan-1-ol **2** (6.5 g, 37.96 mmol) and Et_3N (6.9 mL, 49.34 mmol) in dry THF (25 mL), under an argon atmosphere and at 0 °C, methanesulfonyl chloride (3.8 mL, 49.34 mmol) was added dropwise. After 2 h of stirring at room temperature, the reaction mixture was quenched with saturated NH_4Cl aqueous solution and extracted with CH_2Cl_2 twice. The combined organic layers were then washed with saturated NaCl aqueous solution and dried over anhydrous Na_2SO_4. The solvent was evaporated to give 9.0 g (36.05 mmol, 95% yield) of **3** as a yellow oil, which was used without further purification. R_f = 0.37 (EtOAc/hexanes, 1 : 2); ^{1}H NMR (500 MHz, $CDCl_3$) δ 4.21 (t, 2H, J = 6.6 Hz), 3.25 (t, 2H, J = 7.0 Hz), 3.00 (s, 3H), 1.77–1.71 (m, 2H), 1.61–1.56 (m, 2H), 1.43–1.32 (m, 8H) ppm (Fig. S3†); ^{13}C NMR (125 MHz, $CDCl_3$) δ 70.2, 51.5, 37.5, 29.2, 29.0, 28.9(2), 26.7, 25.4 ppm (Fig. S4†); HRMS (ESI) calcd for $C_9H_{19}O_3N_3NaS$ $(M + Na)^+$: m/z 272.1039, found m/z 272.1038.

2.1.4. 8-Azidooctyl-1-thioacetate (4). To a solution of 8-azidooctyl methanesulfonate **3** (8.5 g, 34.09 mmol), in dry DMF (180 mL), under an argon atmosphere, potassium thioacetate (5.1 g, 44.32 mmol) was added at room temperature. The reaction mixture was stirred overnight, washed with water, and extracted three times with EtOAc. The combined organic phases were washed with saturated $NaHCO_3$ aqueous solution and brine, dried over anhydrous Na_2SO_4 and evaporated, to obtain 7.5 g (32.61 mmol, 96% yield) of **4** as a brown oil, which was used without further purification. R_f = 0.64 (EtOAc/hexanes, 1 : 2); ^{1}H NMR (500 MHz, $CDCl_3$) δ 3.25 (t, 2H, J = 7.0 Hz), 2.86 (t, 2H, J = 7.4 Hz), 2.32 (s, 3H), 1.62–1.53 (m, 4H), 1.37–1.30 (m, 8H) ppm (Fig. S5†); ^{13}C NMR (125 MHz, $CDCl_3$) δ 196.1, 51.6, 30.8, 29.6, 29.2, 29.1 (2), 28.9, 28.8, 26.8 ppm (Fig. S6†); HRMS (ESI) calcd for $C_{10}H_{19}ON_3NaS$ $(M + Na)^+$: m/z 252.1144, found m/z 252.1141.

2.1.5. 8-Azidooctane-1-sulfinyl chloride (5). To a solution of thioacetate **4** (4.0 g, 17.44 mmol) in methylene chloride (15 mL) at −20 °C, acetic anhydride (1.7 mL, 17.44 mmol) and sulfuryl chloride (2.8 mL, 34.88 mmol) were added. The resulting mixture was stirred for 1 h at −5 °C and then the solvent was evaporated and the residue was dried under vacuum to give 4.1 g (17.42 mmol, quantitative yield) of **5** as a black solid with a low melting point. The crude sulfinyl chloride, which was kept under argon, was used without further purification in the following reaction for the preparation of sulfinate esters.

2.1.6. (*S*)-(1,2:5,6-Di-*O*-isopropylidene-α-D-glucofuranosyl) 8-azidooctanesulfinate (6-(*S*)). To a solution of 1,2:5,6-di-*O*-isopropylidene-α-D-glucofuranosyl (DAGOH) (1.5 g, 5.81 mmol) and DIPEA (4.1 mL, 23.25 mmol) in anhydrous toluene (64 mL), cooled to −78 °C and placed under an argon atmosphere, 8-azidooctane-1-sulfinyl chloride **5** (4.1 g, 17.44 mmol) was added while the reaction mixture was vigorously stirred. After stirring at −78 °C for 1 h, the reaction mixture was treated with 1 M HCl aqueous solution and extracted with CH_2Cl_2. The combined organic layers were successively washed with saturated $NaHCO_3$ aqueous solution and brine, dried over Na_2SO_4 and evaporated to obtain the *S* sulfinate as the major diastereomer with a 68 : 32 r.d. The crude product was purified by column chromatography (hexanes/2-propanol, 30 : 1) to give 1.7 g (3.8 mmol, 65% yield) of diastereomerically pure **6-(*S*)** as a yellow oil. R_f = 0.12 (hexanes/2-propanol, 30 : 1); $[\alpha]_D$ = −28.8 (c = 1.6, $CHCl_3$); ^{1}H NMR (500 MHz, $CDCl_3$) δ 5.90 (d, 1H, J = 3.8 Hz), 4.74 (d, 1H, J = 2.6 Hz), 4.60 (d, 1H, J = 3.6 Hz), 4.31–4.26 (m, 2H), 4.09 (dd, 1H, J = 5.8 and 8.4 Hz), 4.00 (dd, 1H, J = 5.1 and 8.4 Hz), 3.26 (t, 2H, J = 6.9 Hz), 2.85–2.72 (m, 2H), 1.74–1.67 (m, 2H), 1.62–1.56 (m, 2H), 1.51 (s, 3H), 1.45–1.30 (m, 17H) ppm (Fig. S7†); ^{13}C NMR (125 MHz, $CDCl_3$) δ 112.6, 109.3, 105.1, 83.8, 80.5, 79.3, 72.6, 66.8, 57.5, 51.5, 29.2, 29.0, 28.9, 28.8, 26.9 (2), 26.7, 26.4, 25.3, 21.4 ppm (Fig. S8†); HRMS (ESI) calcd for $C_{20}H_{35}O_7N_3NaS$ $(M + Na)^+$: m/z 484.2080, found m/z 484.2088.

2.1.7. (*R*)-(−)-1-Azido-8-(methylsulfinyl)-octane (6-(*R*)). To a solution of sulfinate **6-(*S*)** (1.7 g, 3.78 mmol) in anhydrous toluene (20 mL), at 0 °C, 1.4 M methyl magnesium bromide (4.1 mL, 5.66 mmol) was added. After stirring for 1 h at 0 °C, saturated NH_4Cl aqueous solution was added. The aqueous layer was extracted with CH_2Cl_2 and the resulting organic layers were combined, dried on Na_2SO_4, and concentrated. The crude product was purified by column chromatography (hexanes/2-propanol, 5 : 1) to give 622 mg of **6-(*R*)** (2.86 mmol, 76% yield) as a colorless liquid. R_f = 0.14 (hexanes/2-propanol, 5 : 1); $[\alpha]_D$ = −47.6 (c = 1.0, $CHCl_3$); ^{1}H NMR (500 MHz, $CDCl_3$) δ 3.25 (t, 2H, J = 6.9 Hz), 2.75–2.61 (m, 2H), 2.55 (s, 3H), 1.79–1.71 (m, 2H), 1.63–1.54 (m, 2H), 1.53–1.39 (m, 2H), 1.38–1.32 (m, 6H) ppm (Fig. S9†); ^{13}C NMR (125 MHz, $CDCl_3$) δ 54.8, 51.5, 38.7, 29.2, 29.0, 28.9, 28.8, 26.7, 22.7 ppm (Fig. S10†); HRMS (ESI) m/z calcd for $C_9H_{19}ON_3NaS$ $(M + Na)^+$: 240.1144, found: 240.1141.

2.1.8. (*R*)-(−)-1-Isothiocyanato-8-(methylsulfinyl)-octane ((*R*)-8-OITC). To a solution of azide **6-(*R*)** (300 mg, 1.38 mmol) in Et_2O (10.0 mL), triphenylphosphine (688 mg, 2.62 mmol) was added and the reaction was refluxed for 1 h. After removing the solvent under vacuum, carbon disulfide (6.0 mL) was added and the mixture was refluxed for 3 h. Finally, the solvent was removed under vacuum and the crude product was purified by column chromatography (EtOAc/MeOH 20 : 1) to give 194 mg of **(*R*)-8-OITC** (0.83 mmol, 60% yield) as a color-

less liquid. R_f = 0.19 (EtOAc/MeOH, 20 : 1); $[\alpha]_D$ = −51.0 (c = 1.0, $CHCl_3$); ^{1}H NMR (500 MHz, $CDCl_3$) δ 3.50 (t, 2H, J = 6.6 Hz), 2.76–2.62 (m, 2H), 2.56 (s, 3H), 1.81–1.74 (m, 2H), 1.72–1.66 (m, 2H), 1.56–1.31 (m, 8H) ppm (Fig. S11†); ^{13}C NMR (125 MHz, $CDCl_3$) δ 54.8, 45.2, 38.8, 30.0, 29.1, 28.8, 28.6, 26.6, 22.6 ppm (Fig. S12†); HRMS (ESI) m/z calcd for $C_{10}H_{19}ONNaS_2$ $(M + Na)^+$: 256.0800, found: 256.0800; HPLC: ADH Chiralcel column, (*n*-hexane/isopropanol 80 : 20; 0.4 mL min^{-1}; 23 °C) t_R = 26.7 min (*S*-isomer), t_R = 27.9 min (*R*-isomer) (Fig. S13†).

2.2. Animals

Female (25–30 g) Swiss mice were provided from the Animal Production Centre of the University of Seville (Seville, Spain), and kept under constant conditions of both temperature (20–25 °C) and humidity (40–60%) with a 12 hour light/dark cycle. At the Faculty of Pharmacy (University of Seville, Spain), all experiments were performed in accordance with the European Union recommendations (European Council Directive 2012/707/EU) on animal experimentation and following a protocol approved by the Ethics Committee of the University of Seville (23/07/2018/119). Prior to the beginning of the experiments, the mice were acclimatised for a week.

2.3. Primary culture of murine peritoneal macrophages

To perform the primary culture of peritoneal macrophages, the protocol described by Aparicio-Soto *et al.* was adapted.[43] Cell exudate was extracted by intraperitoneal washings with cold sterile Phosphate Buffered Saline (PBS). The collected cells were centrifuged at 3500 rpm, resuspended with RPMI 1640 culture medium supplemented with heat-inactivated fetal calf serum (FCS) (PAA, Pasching, Austria), 100 U mL^{-1} penicillin and 100 mg mL^{-1} streptomycin and L-glutamine (2 mM) and cultured in plates (1×10^6 cells per mL) in the course of 2 hours. After incubation, PBS was used to remove non-adherent cells and the medium was replaced with RPMI 1640 without FCS containing 6.25 or 12.5 μM **(*R*)-8-OITC** or the vehicle (DMSO). After thirty minutes, the immune cells were stimulated with 5 μg mL^{-1} LPS from *Escherichia coli* (Sigma-Aldrich, St Louis, MO, USA) for 18 h. Finally, both the supernatant and the cell pellet were stored at −80 °C by ELISA and western blot assays, respectively.

2.4. Cell viability assay

The sulforhodamine B (SRB) assay was used to determine cell viability.[44] After being cultured with and without the compound of interest for 18 hours, adherent cells (1×10^5 cells per well) were fixed using 50 μL of a trichloroacetic acid solution (50% w/v) (Sigma-Aldrich, St Louis, MO, USA) and incubated at 4 °C for 1 hour. Subsequently, the plates were washed five times with distilled water and allow to air dry. Afterwards, 100 μL of SRB solution (0.4% w/v) (Sigma-Aldrich, St Louis, MO, USA) were added to each well and incubated for 30 minutes at room temperature in the dark. After that time, the supernatant was eliminated, and the plate was washed five times with an acetic acid solution (1% v/v) (Panreac, Barcelona, Spain) and left to air dry. At the end, 100 μL of a Tris base solution (pH 10.5, 10 mmol L^{-1}) (Sigma-Aldrich, St Louis, MO, USA) was added to each well. The optical density (OD) was quantified at 510 nm using a multi-well plate reader spectrophotometer (BioTek, Bad Friedrichshall, Germany) to evaluate the cell survival.

2.5. Measurement of nitric oxide (NO) levels

The Griess reaction assay was used to determine the NO levels. After 18 h of incubation with LPS and **(*R*)-8-OITC**, 100 μL of the supernatant from each well were mixed with 100 μL of the Griess reagent. After incubating for 15 min at room temperature, the OD was determined at 540 nm using an ELISA reader (BioTek, Bad Friedrichshall, Germany).

2.6. Measurement of intracellular ROS levels

Intracellular ROS concentration was quantified using the DCFDA assay kit (Abcam®, Cambridge, UK) following the manufacturer's specifications. The macrophages were plated at a density of 2.5×10^4 cells per well in a black 96-well plate that was pre-treated with **(*R*)-8-OITC** (12.5 and 6.25 μM). Subsequently, after 30 min, the untreated cells as well as the treated cells were activated with LPS. Next, DCFDA (25 μM) was added into each well, which was incubated at 37 °C for 45 min. Both emission and excitation wavelengths (535 and 485 nm, respectively) were measured using a microplate fluorescence reader (Synergy™ HTX®, BioTek, Bad Friedrichshall, Germany).

2.7. Enzyme-linked immunosorbent assay (ELISA)

Supernatants from cultured mouse peritoneal macrophages were processed using ELISA kits to determine the levels of TNF-α and IL-17 (Peprotech®, London, UK), IL-6 (Diaclone®, Besancon Cedex, France) and IL-1β (BD OptEIA®, San Jose, CA, USA) according to the manufacturer's instructions.

2.8. Immunoblotting detection

Proteins obtained from peritoneal macrophages were extracted by scraping and collected in ice-cold PBS supplemented with a mixture of protease and phosphatase inhibitors. The method described by Bradford *et al.* was employed to quantify the protein concentration.[45] Samples with equal amounts of protein (15 μg) were separated by 10% or 15% sodium dodecyl sulphate-polyacrylamide gel electrophoresis (SDS-PAGE) and transferred to a nitrocellulose membrane, followed by blocking it with a blocking solution buffer for 1–2 h at room temperature and incubation overnight at 4 °C with specific primary antibodies (Table 1). After rinsing, the membranes were incubated with a horseradish-peroxidase-labeled anti-mouse antibody (Dako, Atlanta, GA, USA) or an anti-rabbit antibody (Cell Signaling Technology, Danvers, MA, USA) containing blocking solution for 1–2 h at room temperature. The blots were analyzed for β-actin expression in order to prove equal loading. An enhanced chemiluminescence light detection kit was used for immunodetection (Pierce, Rockford, IL, USA). Immune signals were captured using the Amersham Imager 600 from GE

Table 1 Primary antibodies used in western blots

Reference	Antibody target	Host	Dilution	Supplier
13120	iNOS	Rabbit	1 : 1000	Cell Signaling Technology® (Danvers, MA, USA)
9145	pSTAT3	Rabbit	1 : 1000	Cell Signaling Technology® (Danvers, MA, USA)
4511	pp38	Rabbit	1 : 1000	Cell Signaling Technology® (Danvers, MA, USA)
4668	pJNK	Rabbit	1 : 1000	Cell Signaling Technology® (Danvers, MA, USA)
4370	pERK 1/2	Rabbit	1 : 1000	Cell Signaling Technology® (Danvers, MA, USA)
15101	NLRP3	Rabbit	1 : 1000	Cell Signaling Technology® (Danvers, MA, USA)
24232	Caspase 1	Rabbit	1 : 1000	Cell Signaling Technology® (Danvers, MA, USA)
12282	COX-2	Rabbit	1 : 1000	Cell Signaling Technology® (Danvers, MA, USA)
12721	Nrf2	Rabbit	1 : 1000	Cell Signaling Technology® (Danvers, MA, USA)
3771	pJAK2	Rabbit	1 : 1000	Cell Signaling Technology® (Danvers, MA, USA)
9252	JNK	Rabbit	1 : 1000	Cell Signaling Technology® (Danvers, MA, USA)
8690	p38	Rabbit	1 : 1000	Cell Signaling Technology® (Danvers, MA, USA)
9107	ERK 1/2	Mouse	1 : 1000	Cell Signaling Technology® (Danvers, MA, USA)
ab71495	IL-18	Rabbit	1 : 1000	Abcam® (Cambridge, UK)
ab62050	mPGES-1	Rabbit	1 : 1000	Abcam® (Cambridge, UK)
ab49900	β-Actin	Mouse	1 : 10 000	Abcam® (Cambridge, UK)
NBP1-45453	Caspase 11	Rabbit	1 : 500	Novus Biologicals® (Littleton, CO, USA)

Healthcare® (Buckinghamshire, UK). The signals were analyzed and quantified using Image Processing and Analysis in Fiji ImageJ software (W. Rasband, National Institutes of Health) and expressed in relation to the DMSO-LPS control treated cells.

2.9. Statistical evaluation

All values in the figures and text are expressed as arithmetic means ± standard error (SEM). Data were evaluated using GraphPad Prism version 5.01 software (San Diego, CA, USA). One-way analysis of variance (ANOVA) was used to evaluate the statistical significance of any difference in each parameter between groups, and after that, Tukey's multiple comparison test was used as a *post hoc* test. p-Values <0.05 were considered statistically significant.

3. Results

3.1. Synthesis of (*R*)-8-OITC

The synthesis of **(*R*)-8-OITC** was carried out following the "DAG methodology" designed by our group. In this sense, for the synthesis of the desired 1-azidooctanesulfinyl chloride **5**, the treatment of 8-chloro-1-octanol **1** with sodium azide in DMF afforded the azido alcohol **2** in a quantitative yield, which after mesylation gave the azido mesylate intermediate **3** in excellent yield (95%). Treatment of mesylate **3** with sodium thioacetate gave compound **4** in 96% yield. The direct transformation of thioacetate **4** obtained to the desired sulfinyl chloride **5** has been achieved by treatment with sulfuryl chloride and acetic anhydride in methylene chloride (Scheme 1).

According to the "DAG methodology", the treatment of DAG with azidoalkanesulfinyl chloride **5** in the presence of DIPEA gave the (*S*)-sulfinate ester **6-(S_S)** in 65% yield and a good r.d. of 68 : 32.

Taking into account that the reaction of sulfinate ester with Grignard reagents takes place with inversion of configuration at the sulfinyl sulfur, condensation of methyl Grignard on the sulfinate ester **6-(S_S)** provided the corresponding azidoalkyl methyl sulfoxide **7-(R_S)** with the same absolute configuration as natural SFN in 76% yield.

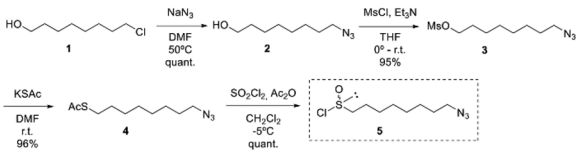

Scheme 1 Synthetic route of (*S*)-(1,2:5,6-di-*O*-isopropylidene-α-D-glucofuranosyl) 8-azidooctanesulfinate (**6-(S_S)**).

Finally, a 2-reaction one-pot sequence based on the Staudinger reaction of an azido derivative with triphenylphosphine and subsequent aza Wittig-type condensation of the resulting iminophosphorane with carbon disulfide led to the first synthesis of enantiomerically pure natural **(*R*)-8-OITC** in a 60% yield (Scheme 2).

3.2. Cell viability of (*R*)-8-OITC on murine peritoneal macrophages

An SRB assay was used to evaluate the cell viability of **(*R*)-8-OITC** on peritoneal macrophages. The concentrations of this ITC (200–1.6 μM) were used for 18 hours to treat immune cells. As shown in Fig. 1, the viability was unaffected between the concentration range of 12.5 to 1.6 μM **(*R*)-8-OITC** (≥80%). As a vehicle, DMSO was used without influencing cell survival. Therefore, we selected 12.5 and 6.25 μM concentrations of **(*R*)-8-OITC** to be studied in the following assays.

3.3. (*R*)-8-OITC lowered nitrite and ROS production and inhibited iNOS and Nrf2 protein expression in LPS-stimulated murine peritoneal macrophages

To study the impact of the treatment with **(*R*)-8-OITC** on the iNOS/NO activated pathway and ROS production produced by LPS stimulation on immune cells, we proceeded to determine the protein expression level of iNOS and NO and ROS pro-

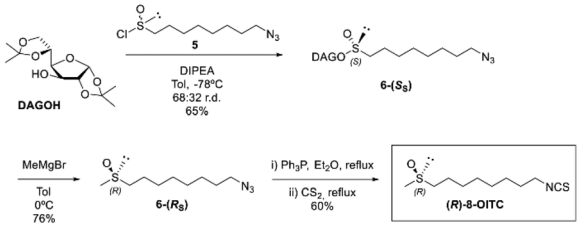

Scheme 2 Synthetic route of **(*R*)-8-OITC** from (*S*)-(1,2:5,6-di-*O*-isopropylidene-α-D-glucofuranosyl) 8-azidooctanesulfinate (**6-(S_S)**).

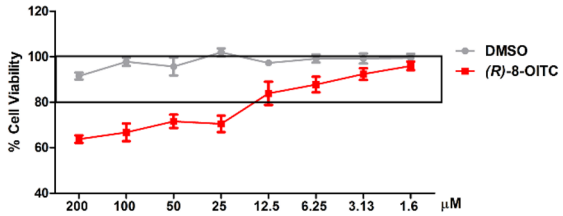

Fig. 1 Effect of **(*R*)-8-OITC** on cell viability. Viability rate was expressed as the percentage of cell survival with respect to 100% of the control untreated cells. Results are presented as mean ± S.E.M. of at least six independent experiments.

duction by western blotting, Griess assay and DCFDA assay, respectively. LPS stimulation produced a statistically significant increase in the levels of NO and ROS as well as the iNOS expression ($^{+++}p < 0.001$ *vs.* the unstimulated control cells) (Fig. 2A, B and C, respectively). On the other hand, treatment with both concentrations (12.5 and 6.25 μM) of **(*R*)-8-OITC** significantly decreased NO and ROS production levels and iNOS protein expression ($^{***}p < 0.001$ *vs.* the LPS-DMSO cells).

In addition, nuclear factor erythroid 2 (Nrf2) is a transcription factor that participates in the cellular response to oxidative stress.[46] A significant up-regulation of Nrf2 protein expression in cells treated with **(*R*)-8-OITC** ($^{*}p < 0.05$ and $^{***}p < 0.001$ *vs.* the LPS-DMSO-treated cells) was seen (Fig. 2D). In summary, all of these data could reveal the potential antioxidant role of **(*R*)-8-OITC**.

3.4. (*R*)-8-OITC decreased IL-17, IL-6, IL-1β and TNF-α cytokine production

Fig. 3 shows a statistically significant increase in the production of IL-17, IL-6, IL-1β and TNF-α cytokines in LPS-stimulated mouse peritoneal macrophages ($^{++}p < 0.01$ and $^{+++}p < 0.001$ *vs.* the unstimulated control cells). However, treatment with **(*R*)-8-OITC** (12.5 and 6.25 μM) was able to reverse these effects in a statistically significant way ($^{***}p < 0.001$ *vs.* the LPS-DMSO stimulated cells).

3.5. (*R*)-8-OITC diminished the protein expression levels of COX-2 and mPGES-1 in LPS-activated murine peritoneal macrophages

The expressions of COX-2 and mPGES-1 were statistically augmented in the LPS-DMSO stimulated control cells in comparison with the unstimulated control cells ($^{+++}p < 0.001$ *vs.* the unstimulated control cells). To investigate whether **(*R*)-8-OITC** could inhibit LPS-induced COX-2 and mPGES-1 protein expressions, murine cells were pretreated with 12.5 and 6.25 μM concentrations of this ITC for 30 min, before stimulating with LPS (5 μg mL^{-1}) for 18 h. **(*R*)-8-OITC** at both concentrations (12.5 and 6.25 μM) significantly reduced the protein expressions of COX-2 and mPGES-1 ($^{***}p < 0.001$ *vs.* the LPS-DMSO-treated cells) (Fig. 4).

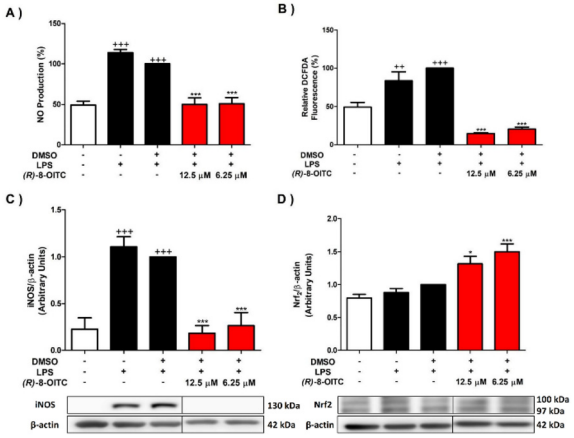

Fig. 2 **(*R*)-8-OITC** treatment decreased the levels of NO (A) and ROS (B) production as well as down-regulated the expression of the pro-inflammatory enzyme iNOS (C) and up-regulated the expression of Nrf2 (D). Murine cells were pretreated for half an hour with **(*R*)-8-OITC** (12.5 or 6.25 μM), and then stimulated with LPS for 18 h. Normalization of densitometry was carried out by measuring the β-actin housekeeping gene. Data shown are means ± S.E.M. (n = 6) ($^{+++}p < 0.001$ *vs.* the control cells (unstimulated); $^{*}p < 0.05$ and $^{***}p < 0.001$ *vs.* the LPS-DMSO cells).

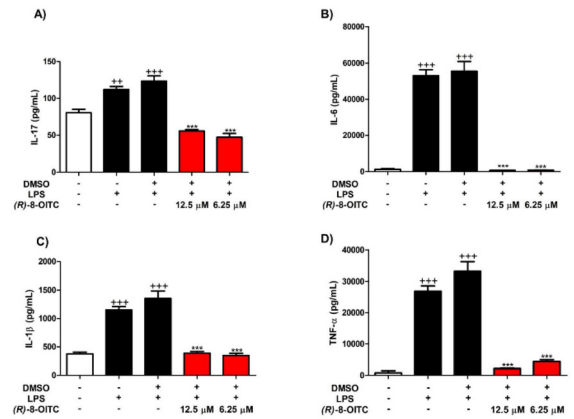

Fig. 3 **(*R*)-8-OITC** diminished IL-17 (A), IL-6 (B), IL-1β (C) and TNF-α (D) pro-inflammatory cytokine production. Immune cells were pretreated with **(*R*)-8-OITC** (12.5 or 6.25 μM) for 30 min. Then, they were stimulated with 5 μg mL^{-1} LPS for 18 h. The level of cytokines was measured by ELISA assays. Data are expressed as mean ± S.E.M. (n = 8) ($^{+++}p < 0.001$ and $^{++}p < 0.01$ *vs.* the control cells (unstimulated); $^{***}p < 0.001$ *vs.* the LPS-DMSO-treated cells).

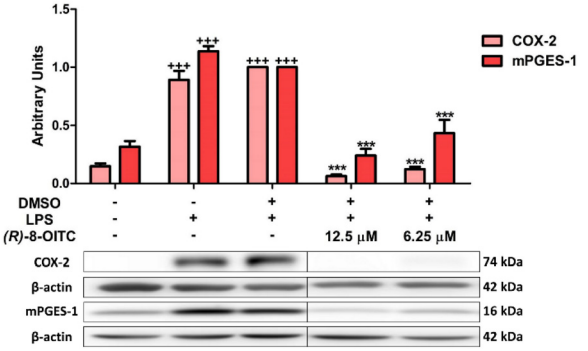

Fig. 4 **(*R*)-8-OITC** downregulated COX-2 and mPGES-1 protein expressions in murine immune cells. COX-2 and mPGES-1 protein expressions were determined by the western blot assay. Normalization of the densitometric analysis was carried out by measuring the β-actin housekeeping gene. Data are represented as means ± S.E.M. (n = 6) ($^{+++}p < 0.001$ *vs.* the control cells (unstimulated); $^{***}p < 0.001$ *vs.* the LPS-DMSO-treated cells).

3.6. JAK/STAT signaling pathway is inhibited by (*R*)-8-OITC in LPS-activated murine peritoneal macrophages

We evaluated whether **(*R*)-8-OITC** could modulate the JAK/STAT signaling pathway. When murine peritoneal macrophages were stimulated with LPS, the levels of phosphorylation of both JAK2 and STAT3 were increased compared to the unstimulated control cells ($^{+++}p < 0.001$ *vs.* the unstimulated control cells). Nevertheless, in the presence of **(*R*)-8-OITC** pretreatment (12.5 and 6.25 μM), a significant decrease of the phosphorylation of JAK2 and STAT3 was observed ($^{*}p < 0.05$, $^{**}p < 0.01$ and $^{***}p < 0.001$ *vs.* the LPS-DMSO-treated cells) (Fig. 5).

3.7. (*R*)-8-OITC reduced MAPK activation in LPS-activated peritoneal macrophages

To evaluate the effects of **(*R*)-8-OITC** on MAPKs (ERK, p38 and JNK) phosphorylation, western blot assays were performed. As

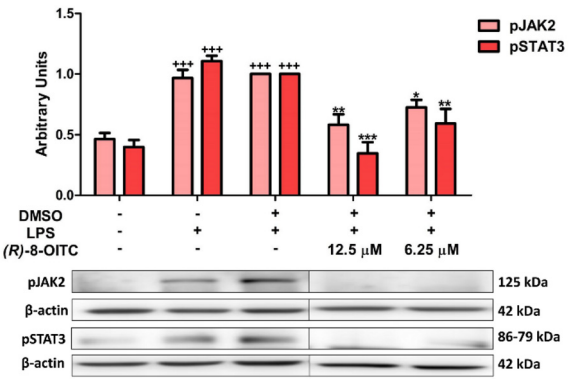

Fig. 5 **(*R*)-8-OITC** decreased the phosphorylation levels of JAK2 and STAT3 on LPS-activated immune cells. Macrophages were pretreated for half an hour with **(*R*)-8-OITC** (12.5 or 6.25 μM), followed by stimulation with LPS (5 μg mL^{-1}) for 18 h. Normalization of the densitometric analysis was carried out by measuring the β-actin housekeeping gene. Data shown are means ± S.E.M. (n = 6) ($^{+++}p < 0.001$ *vs.* the control cells (unstimulated); $^{*}p < 0.05$; $^{**}p < 0.01$ and $^{***}p < 0.001$ *vs.* the LPS-DMSO-treated cells).

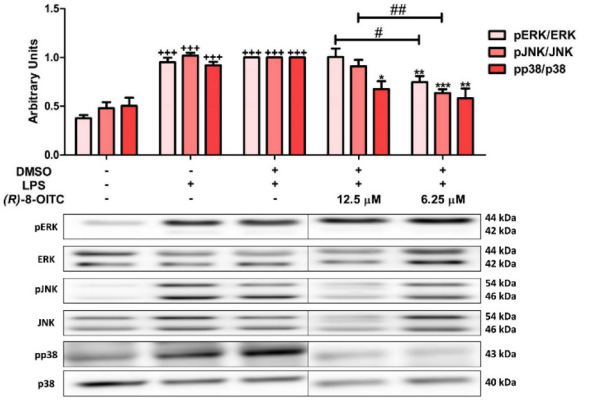

Fig. 6 **(*R*)-8-OITC** reduced the phosphorylation of p38, JNK and ERK on LPS-activated immune cells. Macrophages were pretreated with **(*R*)-8-OITC** (12.5 or 6.25 μM) for 30 min, followed by LPS stimulation for 18 h. Normalization of the densitometric analysis of pp38, pJNK and pERK were carried out by measuring the p38, JNK and ERK housekeeping genes. Data shown are means ± S.E.M. (n = 6) ($^{+++}p < 0.001$ *vs.* the control cells (unstimulated); $^{*}p < 0.05$; $^{**}p < 0.01$ and $^{***}p < 0.001$ *vs.* the LPS-DMSO-treated cells; $^{\#}p < 0.05$ and $^{\#\#}p < 0.01$ *vs.* 12.5 μM **(*R*)-8-OITC**).

can be seen in Fig. 6, the level of phosphorylation of these MAPKs was significantly increased in the LPS-DMSO stimulated control cells ($^{+++}p < 0.001$ *vs.* the unstimulated control cells). After **(*R*)-8-OITC** (12.5 and 6.25 μM) incubation, p38 phosphorylation was statistically decreased ($^{*}p < 0.05$ and $^{**}p < 0.01$ *vs.* the LPS-DMSO-treated cells). However, only 6.25 μM **(*R*)-8-OITC** was able to reduce the phosphorylation of ERK and JNK ($^{**}p < 0.01$ and $^{***}p < 0.001$ *vs.* the LPS-DMSO control cells).

3.8. Canonical and non-canonical inflammasomes were inhibited by treatment with (*R*)-8-OITC in LPS-activated murine peritoneal macrophages

To further investigate the signaling pathways involved in the immunomodulatory effects of **(*R*)-8-OITC** in LPS-activated murine peritoneal macrophages, its role in modulating the canonical and non-canonical pathways of the inflammasome was assessed.

As shown in Fig. 7, when macrophages were exposed to LPS, the protein expressions of NLRP3, caspase 1 and caspase 11 were upregulated ($^{+}p < 0.05$ and $^{+++}p < 0.001$ *vs.* the unstimulated control cells). Nevertheless, the pretreatment with 12.5 or 6.25 μM **(*R*)-8-OITC** could significantly revert the expression levels of these proteins ($^{**}p < 0.01$ and $^{***}p < 0.001$ *vs.* the LPS-DMSO-treated cells). It is noted that 12.5 μM concentration of this compound statistically decreased the expressions of NLRP3 and caspase 1 compared to 6.25 μM ($^{\#\#}p < 0.01$ and $^{\#\#\#}p < 0.001$ *vs.* the cells treated with 6.25 μM **(*R*)-8-OITC**) (Fig. 7A and B, respectively).

As a consequence of the activation of the NLRP3 inflammasome, pro-IL-1β and pro-IL-18 cytokines matured to IL-1β and IL-18. For this reason, we also evaluated the expression levels

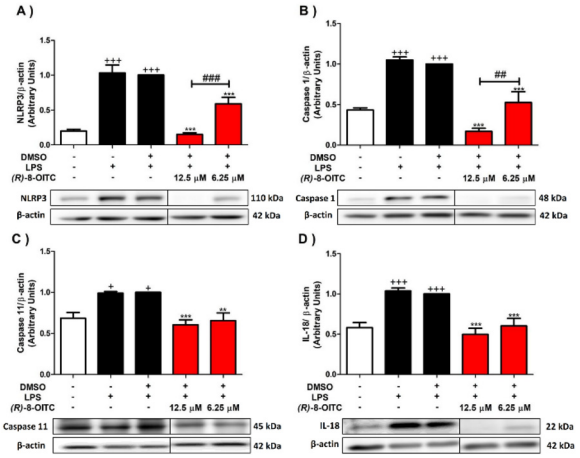

Fig. 7 **(*R*)-8-OITC** decreased the canonical and non-canonical inflammasome signaling pathways in the LPS-stimulated immune cells. Murine peritoneal macrophages were pretreated for half an hour with both concentrations (12.5 or 6.25 μM) of **(*R*)-8-OITC**, followed by stimulation with LPS for 18 h. Normalization of the densitometric analysis of NLRP3 (A), Caspase 1 (B), Caspase 11 (C) and IL-18 (D) was carried out by measuring the β-actin housekeeping gene. Data shown are means ± S.E.M. (n = 6) ($^{+}p < 0.05$ and $^{+++}p < 0.001$ *vs.* the unstimulated control cells; $^{**}p < 0.01$ and $^{***}p < 0.001$ *vs.* the LPS-DMSO-treated cells; $^{\#\#}p < 0.01$ and $^{\#\#\#}p < 0.001$ *vs.* the cells treated with 6.25 μM **(*R*)-8-OITC**).

of these cytokines (Fig. 7D and 3C, respectively). IL-1β and IL-18 levels were augmented in the LPS-stimulated control cells ($^{+++}p < 0.001$ *vs.* the unstimulated control cells). Nevertheless, the cells treated with 12.5 or 6.25 μM concentration of this ITC significantly reduced the production of these cytokines ($^{***}p < 0.001$ *vs.* the LPS-DMSO-treated cells) (Fig. 7D and 3C).

4. Discussion

The results obtained in this research have demonstrated, for the first time, a new simple and high-throughput synthetic route based on the "DAG methodology" for **(*R*)-8-OITC**, as well as demonstrated the immunomodulatory activity of this ITC in an *ex vivo* murine model of peritoneal macrophages stimulated by LPS. To date, the synthesis of the natural ITC **(*R*)-8-OITC** has not been reported in a rapid and cost-effective method, nor is there any data on the anti-inflammatory and antioxidant activity of this active compound.

As an alkyl methyl sulfoxide, the synthesis of enantiopure SFN and its analogues is not straightforward, and the main approximations for the synthesis of enantiomerically pure sulfoxides developed so far fail in the preparation of simple dialkyl sulfoxides.[47–50]

The most direct method for the synthesis of an enantiopure chiral sulfoxide is the enantioselective oxidation of its prochiral thioether.[51] However, there is no asymmetric catalytic oxidation that is able to give enantiomerically pure dialkyl sulfoxides from the corresponding prochiral thioethers and, in the particular case of SFN, the natural enantiomer is obtained as a scalemic compound.[52–54] The method developed by Whitesell allows the enantiopure SFN, but its application to the synthesis of other sulfur substituted analogs is limited.[55] To solve this problem, in 2009, we reported that sulfinate ester **I** is an effective sulfinylating agent capable of efficiently transferring the linear alkyl SFN side chain to different alkyl or aryl groups in an enantiomeric form (Chart 2).[34,56–59]

In the present work, to modulate the carbonated side chain between the sulfoxide and the ITC group and to produce the SFN homologue **(*R*)-8-OITC**, we used the "DAG-methodology", developed by our group. It is the method of choice, as it is able to give a diasteromerically pure sulfinate ester with a non-hindered alkyl chain at the sulfinyl sulfur in addition to synthesizing the natural enantiopure compound in just seven reaction steps from inexpensive starting materials.

Effects derived from LPS stimulated macrophages are enhanced levels of ROS production and the overexpression of the pro-inflammatory enzyme iNOS, responsible for the production of NO, which has important functions in the regulation of the immune system and host defense, acting as a messenger regulating the production of intracellular ROS and leading to redox imbalance.[60–62] Other studies have described that the redox-sensitive transcription factor Nrf2 protects against inflammatory response in macrophages.[63] Under basal conditions, Nrf2 is negatively modulated by Kelch-associated protein 1 (KEAP1), which acts as a substrate adaptor protein for the Cullin 3-RING-based E3 ubiquitin protein ligase and employs a cyclic mechanism to continuously direct Nrf2 toward ubiquitination and proteasomal degradation.[64]

Interestingly, our results show that **(*R*)-8-OITC** treatment decreased iNOS enzyme expression and increased Nrf2 immunosignaling by sequentially reducing NO and ROS production counteracting ROS-induced cell damage. Kim *et al.* reported similar results using allyl ITC (AITC) in LPS-stimulated RAW 264.7 macrophages.[65] Additionally, our group has recently published how the natural ITC (*R*)-SFN was able to decrease iNOS protein expression and, consequently, NO production, and reduce the levels of ROS production[33] in the same *ex vivo* preclinical model.

In this context, other ITCs such as (*R*)-SFN are known activators of Nrf2 by stimulating the nuclear translocation of Nrf2, which can be phosphorylated by the activation of multiple kinases that in turn stimulate the expression of detoxification

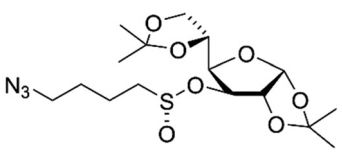

I
Fernández-Khiar[37,59-62]

Chart 2 Diastereomeric intermediate used for the synthesis of enantiopure (*R*)-SFN.

enzymes. Due to its high chemical reactivity, the ITC group can easily interact with the cysteine of glutathione in a reaction catalyzed by glutathione transferases. It has also been suggested that ITC activates Nrf2 by modifying the cysteine residues in KEAP1.[66] Altogether, these data demonstrated the possible antioxidant activity of **(*R*)-8-OITC**. However, additional studies are required to corroborate this pharmacological activity. Furthermore, another ITC which has been shown as an inducer of Nrf2 is AITC in RAW 264.7 macrophages.[67]

In addition, macrophage activation by LPS is closely involved with an imbalance in the cytokine network, which induces the upregulation of several pro-inflammatory Th17 and Th1 cytokines including IL-17, TNF-α, IL-1β and IL-6 among others.[68,69] In line with these observations, our data showed a marked increase in inflammatory cytokine expression after LPS stimulation. Nevertheless, secretion of the cytokines IL-17, TNF-α, IL-1β, IL-6 and IL-18 were significantly reduced by treatment with **(*R*)-8-OITC**. Similar results have been obtained with other ITCs such as racemic SFN and benzyl ITC (BEITC) in LPS-stimulated RAW 264.7 macrophages, (*R*)-SFN in LPS-activated peritoneal murine macrophages and LPS-activated populations in healthy adult volunteers.[33,70–72]

When LPS activates macrophages, inflammatory mediators such as prostaglandin E2, a bioactive signaling molecule whose overproduction is generated by increased expression of COX-2 and mPGES-1, are produced.[73,74]

In agreement with our previous reports, LPS stimulation generated a significant increase in the protein expressions of both COX-2 and mPGES-1.[43,75–77] On the other hand, pre-treatment with **(*R*)-8-OITC** decreased the protein expressions of both pro-inflammatory enzymes significantly, thus reversing the action of LPS. In this regard, other research has shown that other ITCs such as 2-phenylbutyl ITC or SFN are able to inhibit COX-2 overproduction in the macrophage RAW 264.7 cell line and in mouse peritoneal macrophages.[78,79]

To further understand the mechanisms of action of **(*R*)-8-OITC**, the JAK2/STAT3 and MAPK signaling pathways were investigated.

The JAK-STAT signalling pathway is essential for the immune system. JAK2 is a cytoplasmic tyrosine protein kinase that is non-covalently ligated to cytokine receptors. When it is activated, JAK2 recruits and phosphorylates the transcription factor STAT3, leading to its dimerisation and subsequent translocation to the nucleus, where it initiates the transcription of specific genes encoding the transcription of inflammation-related genes, in particular, various chemokines and cytokines.[80] According to our prior research, cell activation by LPS resulted in increased phosphorylation of JAK2 and STAT3 proteins.[33] However, treatment with **(*R*)-8-OITC** significantly decreased the phosphorylation levels of these two proteins. Based on the above, we can suggest that inhibition of the JAK2/STAT3 axis may play an important role in decreasing the production of pro-inflammatory cytokines. This signalling pathway has also been shown to be affected by other ITCs such as 3-methylsulfinylpropyl ITC (iberin) or AITC in a TR146 cell line and in an animal model of DMBA-induced rat mammary tumorigenesis.[81,82]

MAPKs, a family of serine/threonine protein kinases, also play an important role in cell regulation and modulate the expression of several inflammation-related genes such as iNOS, COX-2 and IL-6, among others.[83] This family includes extracellular signal-regulated kinases (ERKs-1 and -2), c-Jun N-terminal kinases (JNKs) and p38, which carry out cascades of reactions that allow them to respond to oxidative and inflammatory stress generated by the stimulus.[84] Consistent with our previous publications, our results indicate that exposure of peritoneal macrophages to LPS resulted in significantly increased levels of ERK, JNK and p38 phosphorylation.[76,85] Nevertheless, **(*R*)-8-OITC** treatment significantly decreased the phosphorylation of ERK, JNK and p38 produced by LPS. Similar results were obtained other ITCs such as (*R*)-SFN and iberin using murine peritoneal macrophages or the RAW 264.7 cell line, respectively, and AITC in LPS-stimulated murine microglial BV2 cells.[33,86,87]

The NLRP3 inflammasome is a supramolecular protein complex that is part of innate immune responses and is stimulated by different pathogen-associated molecular patterns, such as LPS or ROS.[88]

Our previous reports have shown that LPS-induced inflammation triggers stimulation of the NLRP3 inflammasome in macrophages.[75] Although NLRP3 activation can be through two different pathways, canonical and non-canonical, they have the same consequence: pyroptosis and inflammatory cell death. Regarding the canonical pathway, the activated NLRP3 inflammasome recruits the adaptor molecule apoptosis-associated speck-like protein (ASC) to form a complex, the pyroptosome ASC. Subsequently, this complex binds to an effector, pro-caspase 1, which, by autoproteolytic activity, is converted into its active form, caspase 1. This generates the maturation of the pro-inflammatory cytokines IL-18 and IL-1β. On the other hand, the non-canonical pathway is characterized by the maturation of caspase 11, which induces potassium efflux and pyroptosis, triggering the activation of the canonical pathway of the inflammasome.[89]

Accordingly, in the present study, LPS-activated murine peritoneal macrophages resulted in activation of the canonical and non-canonical NLRP3 inflammasome pathways, as there was a significant increase in the protein expressions of NLRP3, caspase 1 and caspase 11 and the production of the pro-inflammatory cytokines IL-1β and IL-18, in agreement with previous studies.[75,76] Other ITCs, such as BEITC and SFN, have been reported to attenuate NLRP3 inflammasome activation in human THP-1 macrophages.[90,91] However, for the first time, we have shown that **(*R*)-8-OITC** treatment was able to inhibit both canonical and non-canonical LPS-stimulated NLRP3 inflammasome activation in mouse peritoneal macrophages.

In summary, the present study has developed a new synthetic route to obtain natural **(*R*)-8-OITC** based on the "DAG methodology" and investigated the different mechanisms involved in its anti-inflammatory and immunomodulatory actions.

5. Conclusions

In conclusion, the present study developed for the first time a new cost-effective and efficient synthetic route to obtain natural ITC **(*R*)-8-OITC** by the "DAG methodology". Additionally, our research has shown, for the first time, that this novel ITC showed excellent anti-inflammatory and antioxidant effects in murine peritoneal macrophages stimulated with LPS. Treatment with **(*R*)-8-OITC** inhibited the levels of pro-inflammatory cytokines (IL-1β, TNF-α, IL-6, IL-17 and IL-18), and intracellular ROS and NO production by reducing the expression of pro-inflammatory enzymes (COX-2, iNOS and mPGES-1) through modulation of the expression of Nrf2, MAPKs (p38, JNK and ERK) and JAK/STAT, and the canonical and non-canonical pathways of the inflammasome. Notwithstanding these promising results, additional *in vivo* studies would be necessary to investigate the immunomodulatory effects of **(*R*)-8-OITC**, which may be a promising nutraceutical molecule suitable for the treatment of several immunoinflammatory diseases.

Author contributions

Conceptualization, C. A-d-l-L. and I. V.; data curation, M. A., C. A-d-l-L. and I. V.; formal analysis, M. A., I. V. and R. R; funding acquisition, C. A-d-l-L. and I. F.; investigation, M. A.; methodology, M. A.; project administration, C. A-d-l-L., I. V., R. R. and I. F; resources, C. A-d-l-L. and I. F.; software, M. A; supervision, I. V., C. A-d-l-L., R. R. and I. F.; validation, M. A. and R. M.-G.; visualization, M. A.; writing – original draft, M. A.; and writing – review and editing, C. A-d-l-L., I. V., R. R. and I. F. All authors have read and agreed to the published version of the manuscript.

Conflicts of interest

There are no conflicts to declare.

Acknowledgements

The authors gratefully acknowledge the assistance of the Center for Technology and Innovation Research, University of Seville (CITIUS), for the NMR and MS facilities. M. Alcarranza and R. Muñoz-García gratefully acknowledge support from the FPU fellowship and financial sponsorship from the Spanish Ministerio de Universidades. This research was funded by the Ministerio de Ciencia, Innovación y Universidades, grant number PID2019-104767RB-I00/AEI/10.13039/501100011033, the Consejería de Transformación Económica, Industria, Conocimiento y Universidad, Junta de Andalucía, grant number P20-01171, by FQM-102 and the Consejería de Economía, Conocimiento, Empresas y Universidad, Junta de Andalucía, grant number 2021/CTS-259 by CTS-259.

References

1 M. Klimek-Szczykutowicz, A. Szopa and H. Ekiert, Chemical composition, traditional and professional use in medicine, application in environmental protection, position in food and cosmetics industries, and biotechnological studies of Nasturtium officinale (watercress) – a review, *Fitoterapia*, 2018, **129**, 283–292.
2 R. Yazdanparast, S. Bahramikia and A. Ardestani, Nasturtium officinale reduces oxidative stress and enhances antioxidant capacity in hypercholesterolaemic rats, *Chem.-Biol. Interact.*, 2008, **172**, 176–184.
3 S. Bahramikia and R. Yazdanparast, Effect of hydroalcoholic extracts of Nasturtium officinale leaves on lipid profile in high-fat diet rats, *J. Ethnopharmacol.*, 2008, **115**, 116–121.
4 C. A. Yaricsha and K. Rissyelly, ACE inhibitory activity, Total phenolic and flavonoid content of watercress (Nasturtium officinale R. Br.) extract, *Pharm. J.*, 2017, **9**, 249–251.
5 J. M. Yuan, I. Stepanov, S. E. Murphy, R. Wang, S. Allen, J. Jensen, L. Strayer, J. Adams-Haduch, P. Upadhyaya, C. Le, M. S. Kurzer, H. H. Nelson, M. C. Yu, D. Hatsukami and S. S. Hecht, Clinical trial of 2-phenethyl isothiocyanate as an inhibitor of metabolic activation of a tobacco-specific lung carcinogen in cigarette smokers, *Cancer Prev. Res.*, 2016, **9**, 396–405.
6 D. A. De Souza, P. M. Costa, R. I. M. A. Ribeiro, P. V. T. Vidigal and F. C. H. Pinto, Daily intake of watercress causes inhibition of experimental Ehrlich tumor growth, *J. Bras. Patol. Med. Lab.*, 2016, **52**, 393–399.
7 P. Rose, Q. Huang, C. N. Ong and M. Whiteman, Broccoli and watercress suppress matrix metalloproteinase-9 activity and invasiveness of human MDA-MB-231 breast cancer cells, *Toxicol. Appl. Pharmacol.*, 2005, **209**, 105–113.
8 L. A. Boyd, M. J. McCann, Y. Hashim, R. N. Bennett, C. I. R. Gill and I. R. Rowland, Assessment of the anti-genotoxic, anti-proliferative, and anti-metastatic potential of crude watercress extract in human colon cancer cells, *Nutr. Cancer*, 2006, **55**, 232–241.
9 Q. Li, M. Zhan, W. Chen, B. Zhao, K. Yang, J. Yang, J. Yi, Q. Huang, M. Mohan, Z. Hou and J. Wang, Phenylethyl isothiocyanate reverses cisplatin resistance in biliary tract cancer cells via glutathionylation-dependent degradation of Mcl-1, *Oncotarget*, 2016, **7**, 10271–10282.
10 S. Shahani, F. Behzadfar, D. Jahani, M. Ghasemi and F. Shaki, Antioxidant and antiinflammatory effects of Nasturtium officinale involved in attenuation of gentamicin induced nephrotoxicity, *Toxicol. Mech. Methods*, 2017, **27**, 107–114.
11 H. Amiri, Volatile constituents and antioxidant activity of flowers, stems and leaves of Nasturtium officinale R. Br, *Nat. Prod. Res.*, 2012, **26**, 109–115.
12 H. Sadgehi, M. Mostafazadeh, M. Naderian, M. J. Barmak, M. S. Talebianpoor and F. Mehraban, In vivo anti-inflammatory properties of aerial parts of Nasturtium officinale, *Pharm. Biol.*, 2014, **52**, 169–174.

13 M. C. Fogarty, C. M. Hughes, G. Burke, J. C. Brown and G. W. Davison, Acute and chronic watercress supplementation attenuates exercise-induced peripheral mononuclear cell DNA damage and lipid peroxidation, *Br. J. Nutr.*, 2013, **109**, 293–301.

14 N. A. Casanova, M. F. Simoniello, M. M. López Nigro and M. A. Carballo, Modulator effect of watercress against cyclophosphamide-induced oxidative stress in mice, *Medicina*, 2017, **77**, 201–206.

15 N. Shakerinasab, M. A. Bejeshk, H. Pourghadamyari, H. Najafipour, M. Eftekhari, J. Mottaghipisheh, N. Omidifar, M. Azizi, M. A. Rajizadeh and A. H. Doustimotlagh, The Hydroalcoholic Extract of Nasturtium officinale Reduces Lung Inflammation and Oxidative Stress in an Ovalbumin-Induced Rat Model of Asthma, *Evid.-Based Complement. Altern. Med.*, 2022, **2022**, 5319237.

16 C. Camponogara, C. R. Silva, I. Brusco, M. Piana, H. Faccin, L. M. de Carvalho, A. Schuch, G. Trevisan and S. M. Oliveira, Nasturtium officinale R. Br. effectively reduces the skin inflammation induced by croton oil via glucocorticoid receptor-dependent and NF-κB pathways without causing toxicological effects in mice, *J. Ethnopharmacol.*, 2019, **229**, 190–204.

17 M. Mostafazadeh, H. Sadeghi, H. Sadeghi, V. Zarezade, A. Hadinia and E. Panahi Kokhdan, Further evidence to support acute and chronic anti-inflammatory effects of Nasturtium officinale, *Res. Pharm. Sci.*, 2022, **17**, 305–314.

18 H. F. Hoseini, A. R. Gohari, S. Saeidnia, N. S. Majd and A. Hadjiakhoondi, The effect of Nasturtium officinale on blood glucose level in diabetic rats, *Pharmacol. Ther.*, 2009, **3**, 866–871.

19 R. Zafar, M. Zahoor, A. Shah and F. Majid, Determination of antioxidants and antibacterial activities, total phenolic, polyphenol and pigment contents in Nasturtium officinale, *Pharmacol. Ther.*, 2017, **1**, 11–18.

20 R. Quezada-Lázaro, E. A. Fernández-Zuñiga, A. García, E. Garza-González, L. Alvarez and M. R. Camacho-Corona, Antimycobacterial compounds from Nasturtium officinale, *Afr. J. Tradit., Complementary Altern. Med.*, 2016, **13**, 31–34.

21 K. Hoshino, H. Akiyama, Y. Goda, A. Tanimura and M. Toyoda, Evaluation of antiallergic effects of extracts from ten kinds of vegetables using three in vitro assay systems, *J. Food Hyg. Soc. Jpn.*, 1998, **39**, 72–77.

22 H. Yehuda, Y. Soroka, M. Zlotkin-Frušić, A. Gilhar, Y. Milner and S. Tamir, Isothiocyanates inhibit psoriasis-related proinflammatory factors in human skin, *Inflammation Res.*, 2012, **61**, 735–742.

23 J. Mohammadi, F. T. Motlagh and N. Mohammadi, The effect of hydroalcoholic extract of watercress on parameters of reproductive and sex hormones on the diabetic rats, *J. Pharm. Sci. Res.*, 2017, **9**, 1334–1338.

24 A. Zeb, Phenolic profile and antioxidant potential of wild watercress (Nasturtium officinale L.), *SpringerPlus*, 2015, **4**, 1–7.

25 X. Ma, Q. Ding, X. Hou and X. You, Analysis of flavonoid metabolites in watercress (Nasturtium officinale R. Br.) and the non-heading Chinese cabbage (brassica rapa ssp. chinensis cv. aijiaohuang) using UHPLC-ESI-MS/MS, *Molecules*, 2021, **26**, 5825.

26 S. S. Kyriakou, V. Tragkola, H. Alghol, I. Anestopoulos, T. Amery, K. Stewart, P. G. Winyard, D. T. Trafalis, R. Franco, A. Pappa and M. I. Panayiotidis, Evaluation of Bioactive Properties of Lipophilic Fractions of Edible and Non-Edible Parts of Nasturtium officinale (Watercress) in a Model of Human Malignant Melanoma Cells, *Pharmaceuticals*, 2022, **15**, 141.

27 S. Kyriakou, D. T. Trafalis, M. V. Deligiorgi, R. Franco, A. Pappa and M. I. Panayiotidis, Assessment of Methodological Pipelines for the Determination of Isothiocyanates Derived from Natural Sources, *Antioxidants*, 2022, **11**, 642.

28 D. Ramirez, A. Abellán-Victorio, V. Beretta, A. Camargo and D. A. Moreno, Functional ingredients from brassicaceae species: Overview and perspectives, *Int. J. Mol. Sci.*, 2020, **21**, 1998.

29 A. Raiola, A. Errico, G. Petruk, D. M. Monti, A. Barone and M. M. Rigano, Bioactive compounds in brassicaceae vegetables with a role in the prevention of chronic diseases, *Molecules*, 2018, **23**, 15.

30 L. Bell, O. O. Oloyede, S. Lignou, C. Wagstaff and L. Methven, Taste and Flavor Perceptions of Glucosinolates, Isothiocyanates, and Related Compounds, *Mol. Nutr. Food Res.*, 2018, **62**, e1700990.

31 J. Jeon, S. J. Bong, J. S. Park, Y. K. Park, M. V. Arasu, N. A. Al-Dhabi and S. U. Park, De novo transcriptome analysis and glucosinolate profiling in watercress (Nasturtium officinale R. Br.), *BMC Genomics*, 2017, **18**, 401.

32 P. Rose, 7-Methylsulfinylheptyl and 8-methylsulfinyloctyl isothiocyanates from watercress are potent inducers of phase II enzymes, *Carcinogenesis*, 2000, **21**, 1983–1988.

33 M. Alcarranza, I. Villegas, R. Muñoz-García, R. Recio, I. Fernández and C. Alarcón-de-la-Lastra, Immunomodulatory Effects of (R)-Sulforaphane on LPS-Activated Murine Immune Cells: Molecular Signaling Pathways and Epigenetic Changes in Histone Markers, *Pharmaceuticals*, 2022, **15**, 966.

34 R. Recio, E. Vengut-Climent, L. G. Borrego, N. Khiar and I. Fernández, *Studies in Natural Products Chemistry*, Elsevier B.V., Amsterdam, 2017.

35 D. X. Hou, M. Fukuda, M. Fujii and Y. Fuke, Induction of NADPH:quinone oxidoreductase in murine hepatoma cells by methylsulfinyl isothiocyanates: methyl chain length-activity study, *Int. J. Mol. Med.*, 2000, **6**, 441–444.

36 I. Fernandez, N. Khiar, J. M. Llera and F. Alcudia, Asymmetric synthesis of alkane- and arenesulfinates of diacetone-D-glucose (DAG): an improved and general route to both enantiomerically pure sulfoxides, *J. Org. Chem.*, 1992, **57**, 6789–6796.

37 I. Fernández and N. Khiar, Recent developments in the synthesis and utilization of chiral sulfoxides, *Chem. Rev.*, 2003, **103**, 3651–3705.

38 Y. Yao, K. Liu, Y. Zhao, X. Hu and M. Wang, Pterostilbene and 4′-Methoxyresveratrol Inhibited Lipopolysaccharide-

Induced Inflammatory Response in RAW264.7 Macrophages, *Molecules*, 2018, **23**, 1148.

39 E. L. Mills, B. Kelly, A. Logan, A. S. H. Costa, M. Varma, C. E. Bryant, P. Tourlomousis, J. H. M. Däbritz, E. Gottlieb, I. Latorre, S. C. Corr, G. McManus, D. Ryan, H. T. Jacobs, M. Szibor, R. J. Xavier, T. Braun, C. Frezza, M. P. Murphy and L. A. O'Neill, Repurposing mitochondria from ATP production to ROS generation drives a pro-inflammatory phenotype in macrophages that depends on succinate oxidation by complex II, *Cell*, 2016, **167**, 457–470.

40 Y. L. Hung, S. H. Fang, S. C. Wang, W. C. Cheng, P. L. Liu, C. C. Su, C. S. Chen, M. Y. Huang, K. F. Hua, K. H. Shen, Y. T. Wang, K. Suzuki and C. Y. Li, Corylin protects LPS-induced sepsis and attenuates LPS-induced inflammatory response, *Sci. Rep.*, 2017, **7**, 46299.

41 S. Li, Q. Dai, S. X. Zhang, Y. Liu, Q. Q. Yu, F. Tan, S. H. Lu, Q. Wang, J. W. Chen, H. Q. Huang, P. Q. Liu and M. Li, Ulinastatin attenuates LPS-induced inflammation in mouse macrophage RAW264.7 cells by inhibiting the JNK/NF-κB signaling pathway and activating the PI3K/Akt/Nrf2 pathway, *Acta Pharmacol. Sin.*, 2018, **39**, 1294–1304.

42 F. Vergara, M. Wenzler, B. G. Hansen, D. J. Kliebenstein, B. A. Halkier, J. Gershenzon and B. Schneider, Determination of the absolute configuration of the glucosinolate methyl sulfoxide group reveals a stereospecific biosynthesis of the side chain, *Phytochemistry*, 2008, **69**, 2737–2742.

43 M. Aparicio-Soto, S. Sánchez-Fidalgo, A. González-Benjumea, I. Maya, J. G. Fernández-Bolaños and C. Alarcón-de-la-Lastra, Naturally occurring hydroxytyrosol derivatives: Hydroxytyrosyl acetate and 3,4-dihydroxyphenylglycol modulate inflammatory response in murine peritoneal macrophages. potential utility as new dietary supplements, *J. Agric. Food Chem.*, 2015, **63**, 836–846.

44 P. Skehan, R. Storeng, D. Scudiero, A. Monks, J. McMahon, D. Vistica, J. T. Warren, H. Bokesch, S. Kenney and M. R. Boyd, New Colorimetric Cytotoxicity Assay for Anticancer-Drug Screening, *J. Natl. Cancer Inst.*, 1990, **82**, 1107–1112.

45 M. M. Bradford, A Rapid and Sensitive Method for the Quantitation of Microgram Quantities of Protein Utilizing the Principle of Protein-Dye Binding, *Anal. Biochem.*, 1976, **72**, 248–254.

46 S. L. Kim, H. S. Choi, Y. C. Ko, B. S. Yun and D. S. Lee, 5-Hydroxymaltol Derived from Beetroot Juice through Lactobacillus Fermentation Suppresses Inflammatory Effect and Oxidant Stress via Regulating NF-kB, MAPKs Pathway and NRF2/HO-1 Expression, *Antioxidants*, 2021, **10**, 1324.

47 F. Rebiere, L. Ricard and H. B. Kagan, A General Route to Enantiomerically Pure Sulfoxides from a Chiral Sulfite, *J. Org. Chem.*, 1991, **56**, 5991–5999.

48 M. A. M. Capozzi, C. Cardellicchio, F. Naso and V. Rosito, A straightforward enantioselective route to dialkyl sulfoxides based upon two carbon-for-carbon substitution reactions on the sulfinyl group, *J. Org. Chem.*, 2002, **67**, 7289–7294.

49 J. L. García Ruano, C. Alemparte, M. T. Aranda and M. M. Zarzuelo, A General and Expeditious One-Pot Synthesis of Sulfoxides in High Optical Purity from Norephedrine-Derived Sulfamidites, *Org. Lett.*, 2003, **5**, 75–78.

50 Z. Han, D. Krishnamurthy, P. Grover, H. S. Wilkinson, Q. K. Fang, X. Su, Z. H. Lu, D. Magiera and C. H. Senanayake, A highly selective and practical method for enantiopure sulfoxides utilizing activated and functionally differentiated N-sulfonyl-1,2,3-oxathiazolidine-2-oxide derivatives, *Angew. Chem., Int. Ed.*, 2003, **42**, 2032–2035.

51 J. Legros, J. R. Dehli and C. Bolm, Applications of catalytic asymmetric sulfide oxidations to the syntheses of biologically active sulfoxides, *Adv. Synth. Catal.*, 2005, **347**, 19–31.

52 H. L. Holland, F. M. Brown, B. G. Larsen and M. Zabic, Biotransformation of organic sulfides. Part 7. Formation of chiral isothiocyanato sulfoxides and related compounds by microbial biotransformation, *Tetrahedron: Asymmetry*, 1995, **6**, 1569–1574.

53 W. A. Schenk and M. Dürr, Synthesis of (R)-Sulforaphane Using [cpru(R,R)-CHIRAPHOS]$^+$ as Chiral Auxiliary, *Chem. – Eur. J.*, 1997, **3**, 713–716.

54 G. R. De Nicola, P. Rollin, E. Mazzon and R. Iori, Novel gram-scale production of enantiopure R-Sulforaphane from tuscan black kale seeds, *Molecules*, 2014, **19**, 6975–6986.

55 J. K. Whitesell and M.-S. Wong, Asymmetric Synthesis of Chiral Sulfinate Esters and Sulfoxides. Synthesis of Sulforaphane, *J. Org. Chem.*, 1994, **59**, 597–601.

56 N. Khiar, I. Fernández and R. Recio, WO2013132124A1, 2013.

57 E. Elhalem, R. Recio, S. Werner, F. Lieder, J. M. Calderón-Montaño, M. López-Lázaro, I. Fernández and N. Khiar, Sulforaphane homologues: Enantiodivergent synthesis of both enantiomers, activation of the Nrf2 transcription factor and selective cytotoxic activity, *Eur. J. Med. Chem.*, 2014, **87**, 552–563.

58 R. Recio, E. Elhalem, J. M. Benito, I. Fernández and N. Khiar, NMR study on the stabilization and chiral discrimination of sulforaphane enantiomers and analogues by cyclodextrins, *Carbohydr. Polym.*, 2018, **187**, 118–125.

59 N. Khiar, S. Werner, S. Mallouk, F. Lieder, A. Alcudia and I. Fernández, Enantiopure sulforaphane analogues with various substituents at the sulfinyl sulfur: Asymmetric synthesis and biological activities, *J. Org. Chem.*, 2009, **74**, 6002–6009.

60 L. Li, U. Maitra, N. Singh and L. Gan, Molecular mechanism underlying LPS–induced generation of reactive oxygen species in macrophages, *FASEB J.*, 2010, **24**, 422.3–422.3.

61 M. Canton, R. Sánchez-Rodríguez, I. Spera, F. C. Venegas, M. Favia, A. Viola and A. Castegna, Reactive Oxygen Species in Macrophages: Sources and Targets, *Front. Immunol.*, 2021, **12**, 734229.

62 Q. Xue, Y. Yan, R. Zhang and H. Xiong, Regulation of iNOS on immune cells and its role in diseases, *Int. J. Mol. Sci.*, 2018, **19**, 3805.

63 D. W. Lim, H. J. Choi, S. D. Park, H. Kim, G. R. Yu, J. E. Kim and W. H. Park, Activation of the Nrf2/HO-1 Pathway by Amomum villosum Extract Suppresses LPS-Induced Oxidative Stress in Vitro and *Ex vivo*, *Evid.-Based Complement. Altern. Med.*, 2020, **2020**, 2837853.

64 L. Baird, D. Llères, S. Swift and A. T. Dinkova-Kostova, Regulatory flexibility in the Nrf2-mediated stress response is conferred by conformational cycling of the Keap1-Nrf2 protein complex, *Proc. Natl. Acad. Sci. U. S. A.*, 2013, **110**, 15259–15264.

65 S. J. Kim, H. J. Park and H. S. Youn, Allyl isothiocyanate suppresses lipopolysaccharide-induced expression of inducible nitric oxide synthase, but not induced expression of cyclooxygenase-2, *Mol. Cell. Toxicol.*, 2012, **8**, 149–154.

66 S. Dayalan Naidu, T. Suzuki, M. Yamamoto, J. W. Fahey and A. T. Dinkova-Kostova, Phenethyl Isothiocyanate, a Dual Activator of Transcription Factors NRF2 and HSF1, *Mol. Nutr. Food Res.*, 2018, **62**, 1700908.

67 A. E. Wagner, C. Boesch-Saadatmandi, J. Dose, G. Schultheiss and G. Rimbach, Anti-inflammatory potential of allyl-isothiocyanate-role of Nrf2, NF-κB and microRNA-155, *J. Cell. Mol. Med.*, 2012, **16**, 836–843.

68 Y. H. Jeong, Y. C. Oh, W. K. Cho, N. H. Yim and J. Y. Ma, Hoveniae semen seu fructus ethanol extract exhibits anti-inflammatory activity via MAPK, AP-1, and STAT signaling pathways in LPS-stimulated RAW 264.7 and mouse peritoneal macrophages, *Mediators Inflammation*, 2019, **2019**, 9184769.

69 H. Tang, P. Roy, Q. Di, X. Ma, Y. Xiao, Z. Wu, J. Quan, J. Zhao, W. Xiao and W. Chen, Synthesis compound XCR-7a ameliorates LPS-induced inflammatory response by inhibiting the phosphorylation of c-Fos, *Biomed. Pharmacother.*, 2022, **145**, 112468.

70 R. T. Ruhee, S. Ma and K. Suzuki, Sulforaphane protects cells against lipopolysaccharide-stimulated inflammation in murine macrophages, *Antioxidants*, 2019, **8**, 577.

71 J. Liang, B. Jahraus, E. Balta, J. D. Ziegler, K. Hübner, N. Blank, B. Niesler, G. H. Wabnitz and Y. Samstag, Sulforaphane inhibits inflammatory responses of primary human T-cells by increasing ROS and depleting glutathione, *Front. Immunol.*, 2018, **9**, 2584.

72 Y. M. Lee, M. R. Seon, H. J. Cho, J. S. Kim and J. H. Park, Benzyl isothiocyanate exhibits anti-inflammatory effects in murine macrophages and in mouse skin, *J. Mol. Med.*, 2009, **87**, 1251–1261.

73 E. Moita, A. Gil-Izquierdo, C. Sousa, F. Ferreres, L. R. Silva, P. Valentão, R. Domínguez-Perles, N. Baenas and P. B. Andrade, Integrated Analysis of COX-2 and iNOS Derived Inflammatory Mediators in LPS-Stimulated RAW Macrophages Pre-Exposed to Echium plantagineum L. Bee Pollen Extract, *PLoS One*, 2013, **8**, e59131.

74 J. A. Mitchell, S. Larkin and T. J. Williams, Cyclooxygenase-2: Regulation and Relevance in Inflammation, *Biochem. Pharmacol.*, 1995, **50**, 1535–1542.

75 T. Montoya, M. Aparicio-Soto, M. L. Castejón, M. Á. Rosillo, M. Sánchez-Hidalgo, P. Begines, J. G. Fernández-Bolaños and C. Alarcón-de-la-Lastra, Peracetylated hydroxytyrosol, a new hydroxytyrosol derivate, attenuates LPS-induced inflammatory response in murine peritoneal macrophages via regulation of non-canonical inflammasome, Nrf2/HO1 and JAK/STAT signaling pathways, *J. Nutr. Biochem.*, 2018, **57**, 110–120.

76 T. Montoya, M. L. Castejón, M. Sánchez-Hidalgo, A. González-Benjumea, J. G. Fernández-Bolaños and C. Alarcón De-La-Lastra, Oleocanthal Modulates LPS-Induced Murine Peritoneal Macrophages Activation via Regulation of Inflammasome, Nrf-2/HO-1, and MAPKs Signaling Pathways, *J. Agric. Food Chem.*, 2019, **67**, 5552–5559.

77 M. Aparicio-Soto, C. Alarcón-De-La-Lastra, A. Cárdeno, S. Sánchez-Fidalgo and M. Sanchez-Hidalgo, Melatonin modulates microsomal PGE synthase 1 and NF-E2-related factor-2-regulated antioxidant enzyme expression in LPS-induced murine peritoneal macrophages, *Br. J. Pharmacol.*, 2014, **171**, 134–144.

78 S. S. S. Boyanapalli, X. Paredes-Gonzalez, F. Fuentes, C. Zhang, Y. Guo, D. Pung, C. L. L. Saw and A. N. T. Kong, Nrf2 knockout attenuates the anti-inflammatory effects of phenethyl isothiocyanate and curcumin, *Chem. Res. Toxicol.*, 2014, **27**, 2036–2043.

79 K. J. Woo and T. K. Kwon, Sulforaphane suppresses lipopolysaccharide-induced cyclooxygenase-2 (COX-2) expression through the modulation of multiple targets in COX-2 gene promoter, *Int. Immunopharmacol.*, 2007, **7**, 1776–1783.

80 X. Hu, J. li, M. Fu, X. Zhao and W. Wang, The JAK/STAT signaling pathway: from bench to clinic, *Signal Transduction Targeted Ther.*, 2021, **6**, 402.

81 Y. Hosokawa, I. Hosokawa, M. Shimoyama, A. Fujii, J. Sato, K. Kadena, K. Ozaki and K. Hosaka, The Anti-Inflammatory Effects of Iberin on TNF-α-Stimulated Human Oral Epithelial Cells: In Vitro Research, *Biomedicines*, 2022, **10**, 3155.

82 T. Rajakumar and P. Pugalendhi, Allyl isothiocyanate inhibits invasion and angiogenesis in breast cancer via EGFR-mediated JAK-1/STAT-3 signaling pathway, *Amino Acids*, 2023, DOI: **10.1007/s00726-023-03285-2**.

83 Q. Chen, C. Che, S. Yang, P. Ding, M. Si and G. Yang, Anti-inflammatory effects of extracellular vesicles from Morchella on LPS-stimulated RAW264.7 cells via the ROS-mediated p38 MAPK signaling pathway, *Mol. Cell. Biochem.*, 2023, **478**, 317–327.

84 J. S. C. Arthur and S. C. Ley, Mitogen-activated protein kinases in innate immunity, *Nat. Rev. Immunol.*, 2013, **13**, 679–692.

85 R. Muñoz-García, M. Sánchez-Hidalgo, T. Montoya, M. Alcarranza, J. Ortega-Vidal, J. Altarejos and C. Alarcón-de-la-Lastra, Effects of Oleacein, a New Epinutraceutical Bioproduct from Extra Virgin Olive Oil, in LPS-Activated Murine Immune Cells, *Pharmaceuticals*, 2022, **15**, 1338.

86 T. Shibata, F. Nakashima, K. Honda, Y. J. Lu, T. Kondo, Y. Ushida, K. Aizawa, H. Suganuma, S. Oe, H. Tanaka, T. Takahashi and K. Uchida, Toll-like receptors as a target

of food-derived anti-inflammatory compounds, *J. Biol. Chem.*, 2014, **289**, 32757–32772.

87 L. Subedi, R. Venkatesan and S. Y. Kim, Neuroprotective and Anti-Inflammatory Activities of Allyl Isothiocyanate through Attenuation of JNK/NF-κB/TNF-α Signaling, *Int. J. Mol. Sci.*, 2017, **18**, 1423.

88 B. I. Arioz, B. Tastan, E. Tarakcioglu, K. U. Tufekci, M. Olcum, N. Ersoy, A. Bagriyanik, K. Genc and S. Genc, Melatonin attenuates LPS-induced acute depressive-like behaviors and microglial NLRP3 inflammasome activation through the SIRT1/Nrf2 pathway, *Front. Immunol.*, 2019, **10**, 1511.

89 H. M. Blevins, Y. Xu, S. Biby and S. Zhang, The NLRP3 Inflammasome Pathway: A Review of Mechanisms and Inhibitors for the Treatment of Inflammatory Diseases, *Front. Aging Neurosci.*, 2022, **14**, 879021.

90 W. S. Park, J. Lee, G. Na, S. Park, S. K. Seo, J. S. Choi, W. K. Jung and I. W. Choi, Benzyl Isothiocyanate Attenuates Inflammasome Activation in Pseudomonas aeruginosa LPS-Stimulated THP-1 Cells and Exerts Regulation through the MAPKs/NF-κB Pathway, *Int. J. Mol. Sci.*, 2022, **23**, 1228.

91 Y. W. An, K. A. Jhang, S. Y. Woo, J. L. Kang and Y. H. Chong, Sulforaphane exerts its anti-inflammatory effect against amyloid-β peptide via STAT-1 dephosphorylation and activation of Nrf2/HO-1 cascade in human THP-1 macrophages, *Neurobiol. Aging*, 2016, **38**, 1–10.